

Molecular characterization and clinical outcome of B-cell precursor acute lymphoblastic leukemia with *IG-MYC* rearrangement

Simon Bomken,^{1,2*} Amir Enshaei,¹ Edward C. Schwalbe,³ Aneta Mikulasova,⁴ Yunfeng Dai,⁵ Masood Zaka,^{6,7} Kent T.M. Fung,¹ Matthew Bashton,⁸ Huezin Lim,¹ Lisa Jones,¹ Nefeli Karataraki,^{1,4} Emily Winterman,¹ Cody Ashby,⁹ Andishe Attarbaschi,¹⁰ Yves Bertrand,¹¹ Jutta Bradtke,¹² Barbara Buldini,¹³ G.A. Amos Burke,¹⁴ Giovanni Cazzaniga,^{15,16} Gudrun Göhring,¹⁷ Hesta A. de Groot-Kruseman,^{18,19} Claudia Haferlach,²⁰ Luca Lo Nigro,²¹ Mayur Parihar,²² Adriana Plesa,²³ Emma Seaford,²⁴ Edwin Sonneveld,¹⁹ Sabine Strehl,²⁵ Vincent H.J. van der Velden,²⁶ Vikki Rand,^{6,7} Stephen P. Hunger,²⁷ Christine J. Harrison,¹ Chris M. Bacon,^{1,2} Frederik W. van Delft,^{1,2} Mignon L. Loh,²⁸ John Moppett,²⁴ Josef Vormoor,^{1,19°} Brian A. Walker,²⁹ Anthony V. Moorman¹ and Lisa J. Russell^{1,4*}

¹Wolfson Childhood Cancer Centre, Translational and Clinical Research Institute, Newcastle University, Newcastle upon Tyne, UK; ²The Great North Children's Hospital, Newcastle upon Tyne Hospitals NHS Foundation Trust, Newcastle upon Tyne, UK; ³Department of Applied Sciences, Northumbria University, Newcastle upon Tyne, UK; ⁴Biosciences Institute, Newcastle University, Newcastle upon Tyne, UK; ⁵Department of Biostatistics, Colleges of Medicine, Public Health and Health Professions, University of Florida, Gainesville, FL, USA; ⁶School of Health and Life Sciences, Teesside University, Middlesbrough, UK; ⁷National Horizons Centre, Teesside University, Darlington, UK; ⁸The Hub for Biotechnology in the Built Environment, Faculty of Health and Life Sciences, Northumbria University, Newcastle upon Tyne, UK; ⁹Department of Biomedical Informatics / Cancer Institute, University of Arkansas for Medical Sciences, Little Rock, AR, USA; ¹⁰St Anna Children's Hospital, Medical University of Vienna, Vienna, Austria; ¹¹Department of Institute of Hematology Oncology Pediatric (IHOP), Hospices Civils de Lyon, Lyon, France; ¹²Institute of Pathology, Department Cytogenetics, University Hospital Giessen and Marburg, Giessen, Germany; ¹³Maternal and Child Health Department, Padua University, Padua Italy; ¹⁴Department of Paediatric Haematology, Oncology, and Palliative Care, Cambridge University Hospitals NHS Foundation Trust, Addenbrooke's Hospital, Cambridge, UK; ¹⁵School of Medicine and Surgery, University of Milano-Bicocca, Monza, Italy; ¹⁶Centro Ricerca Tettamanti, University of Milano-Bicocca, Monza, Italy; ¹⁷Department of Human Genetics, Hannover Medical School, Hannover, Germany; ¹⁸Dutch Childhood Oncology Group (DCOG), Utrecht, the Netherlands; ¹⁹Princess Máxima Center for Pediatric Oncology, Utrecht, the Netherlands; ²⁰MLL Munich Leukemia Laboratory, Munich, Germany; ²¹Cytogenetic-Cytofluorimetric-Molecular Biology Laboratory, Center of Pediatric Hematology Oncology, Azienda Policlinico "G. Rodolico - San Marco", Catania, Italy; ²²Department of Cytogenetics and Laboratory Haematology, Tata Medical Centre, Kolkata, India; ²³Hematology and Flow cytometry Laboratory, Lyon Sud University Hospital, Hospices Civils de Lyon, Lyon, France; ²⁴Department of Paediatric Oncology, Bristol Royal Hospital for Children, Bristol, UK; ²⁵St. Anna Children's Cancer Research Institute (CCRI), Vienna, Austria; ²⁶Department of Immunology, Erasmus MC, University Medical Center Rotterdam, Rotterdam, the Netherlands; ²⁷Department of Pediatrics and the Center for Childhood Cancer Research, Children's Hospital of Philadelphia and the Perelman School of Medicine, University of Pennsylvania, Philadelphia, PA, USA; ²⁸Department of Pediatrics, Benioff Children's Hospital and the Helen Diller Family Comprehensive Cancer Center, University of California, San Francisco, CA, USA and ²⁹Melvin and Bren Simon Comprehensive Cancer Center, Division of Hematology Oncology, Indiana University, Indianapolis, IN, USA

*SB and LJR contributed equally to this work.

°current address University Medical Center Utrecht, Utrecht, the Netherlands

Correspondence: L.J. Russell
lisa.russell@newcastle.ac.uk

S. Bomken
s.n.bomken@newcastle.ac.uk

Received: January 6, 2022.

Accepted: March 31, 2022.

Early view: April 28, 2022.

<https://doi.org/10.3324/haematol.2021.280557>

©2023 Ferrata Storti Foundation

Published under a CC BY license 

Abstract

Rarely, immunophenotypically immature B-cell precursor acute lymphoblastic leukemia (BCP-ALL) carries an immunoglobulin-*MYC* rearrangement (*IG-MYC-r*). This can result in diagnostic confusion with Burkitt lymphoma/leukemia and use of individualized treatment schedules of unproven efficacy. Here we compare the molecular characteristics of these conditions and investigate historic clinical outcome data. We identified 90 cases registered in a national BCP-ALL clinical trial/registry. When present, diagnostic material underwent cytogenetic, exome, methylome and transcriptome analyses. The outcomes analyzed were 3-year event-free survival and overall survival. *IG-MYC-r* was identified in diverse cytogenetic backgrounds, co-existing with either established BCP-ALL-specific abnormalities (high hyperdiploidy, $n=3$; *KMT2A*-rearrangement, $n=6$; *iAMP21*, $n=1$; *BCR-ABL1*, $n=1$); *BCL2/BCL6*-rearrangements ($n=15$); or, most commonly, as the only defining feature ($n=64$). Within this final group, precursor-like V(D)J breakpoints predominated (8/9) and *KRAS* mutations were common (5/11). DNA methylation identified a cluster of V(D)J-rearranged cases, clearly distinct from Burkitt leukemia/lymphoma. Children with *IG-MYC-r* within that subgroup had a 3-year event-free survival of 47% and overall survival of 60%, representing a high-risk BCP-ALL. To develop effective management strategies this group of patients must be allowed access to contemporary, minimal residual disease-adapted, prospective clinical trial protocols.

Introduction

Immunoglobulin (IG)-driven overexpression of the oncogene *MYC* is the genetic hallmark of mature, germinal center-derived Burkitt lymphoma (BL). However, *IG-MYC* translocations are observed in other mature B-cell malignancies including 5-14% of diffuse large B-cell lymphomas, high-grade B-cell lymphomas with *BCL2*-rearrangement (*BCL2-r*) and/or *BCL6*-rearrangement (*BCL6-r*), and multiple myeloma.¹⁻⁵ High *MYC* expression is driven by juxtaposition to powerful *IG* super-enhancers, most commonly the heavy chain locus resulting from the translocation, t(8;14)(q24;q32), but alternatively kappa or lambda light chain loci in the translocations t(2;8)(p11;q24) and t(8;22)(q24;q11), respectively.

Much less commonly, *IG-MYC* rearrangements (*IG-MYC-r*) have been identified in lymphoid malignancies expressing a surface immunoglobulin-negative, immature B-cell precursor (BCP) immunophenotype.⁶⁻¹³ Several recent clinical trials of acute lymphoblastic leukemia (ALL) have excluded these patients to avoid the risk of mistreating mature B-cell non Hodgkin lymphomas (B-NHL). However, a large RNA sequencing study recently identified a distinct group of 18/1,988 (0.9%) BCP-ALL cases characterized by *IG* translocations with either *BCL2*, *BCL6* and/or *MYC*,¹⁴ while a Nordic population-based study estimated the frequency of *IG-MYC-r* in childhood BCP-ALL at 0.6%.¹⁵

Despite the rarity of these conditions, knowing whether to diagnose and treat them as an ALL or Burkitt leukemia/lymphoma is important, with the relevant therapies being markedly different. A recent molecular study of 12 patients demonstrated genetic/epigenetic similarities to BCP-ALL.¹⁶ In contrast, a retrospective clinical study of 14 cases registered with the German BFM-NHL group encouraged treatment according to a mature B-NHL protocol.¹⁷ Clearly there is no current consensus, with many reported

patients receiving hybrid protocols outside the clinical trial setting.^{17,18}

Here, we studied the molecular and clinical characteristics of a cohort of 90 BCP-ALL cases, enrolled in large national clinical trials/registries. Combining cytogenetic characteristics, somatic mutations, DNA methylation and gene expression analysis, we addressed the question of which disease precursor B-cell *IG-MYC-r* leukemias represent - BCP-ALL or BL. We further sought to determine the prognostic implications of the presence of an *IG-MYC-r*. We found that *IG-MYC-r* was present in diverse cytogenetic backgrounds and defined three subgroups within our cohort: (i) cases with *IG-MYC-r* and a cytogenetic abnormality recurrently seen in BCP-ALL; (ii) cases with *IG-MYC-r* and *BCL2-r/BCL6-r*; and (iii) the majority of cases, with *IG-MYC-r* as the defining cytogenetic abnormality. We demonstrate that *IG-MYC-r* can be either the candidate driver event or a secondary cytogenetic feature. We provide further evidence that the majority are distinct from BL and instead represent a subtype of BCP-ALL with a high risk of early relapse. To improve the care of these patients, clinical outcomes should now be assessed in the setting of prospective minimal residual disease-adapted clinical trials.

Methods

Sample cohort

Patients were identified by the UK Leukaemia Research Cytogenetics Group (LRCG), US Children's Oncology Group (COG), Dutch Children's Oncology Group (DCOG) or International Berlin-Frankfurt-Münster (BFM) study group members. The patients' full characteristics, immunophenotype and additional methodological details are included in the *Online Supplementary Data*, *Online Supplementary Tables S1 and S2* and *Online Supplementary Figure S1*. The

primary inclusion criteria were enrollment/registration in a BCP-ALL clinical trial/registry and *IG-MYC-r* detected by karyotyping or fluorescence *in situ* hybridization (FISH) as a translocation involving an immunoglobulin locus (*IG*) and *MYC*: *IGH-MYC-r*, t(8;14)(q24;q32); *IGK-MYC-r*, t(2;8)(p11;q24); *IGL-MYC-r*, t(8;22)(q24;q11). We also identified two patients with T-cell receptor (*TCR*) translocations to the *MYC* locus. Non-trial cases were identified from local/national registries based on a local diagnostic immunophenotype of B-cell precursor malignancy. Children were defined as those patients under the age of 18 years at diagnosis. Informed consent and institutional review board approval were obtained at each collaborating center. This study was performed in accordance with the Declaration of Helsinki.

Conventional cytogenetics and fluorescence *in situ* hybridization

Fixed cells were available for 65 *MYC*-rearranged patients (Online Supplementary Table S1). *IGH*, *IGK*, *IGL*, *MYC*, *BCL2* and *BCL6* FISH studies were performed in all cases with sufficient available cells, in that order of priority. The labeling, capture and scoring methods are described in the Online Supplementary Methods.

Multiplex ligation-dependent probe amplification

Copy number alterations were determined by multiplex ligation-dependent probe amplification (MLPA) using the SALSA MLPA kit P335 (MRC Holland, Amsterdam, the Netherlands) in 27 patients.¹⁹ The kit includes probes to *IKZF1*, *CDKN2A/B*, *PAX5*, *EBF1*, *ETV6*, *BTG1*, *RB1* and *CSF2RA/IL3RA/CRLF2*.

Targeted sequencing

DNA from 17 patients was prepared and sequenced using a targeted next-generation approach to identify translocation breakpoints at *IG* and *MYC* loci, as described previously.⁴ BWA-MEM (v0.7.12) and genome assembly GRCh37 was used for sequence mapping. Chromosomal rearrangements were called using Manta (v.0.29.6)^{4,20} and manually inspected in Integrative Genomics Viewer (Broad Institute, Cambridge, MA, USA).

Whole exome sequencing

DNA libraries of 15 diagnostic and two relapse samples were generated using the TWIST Human Core Exome kit (Twist Biosciences, San Francisco, CA, USA) and paired end sequencing performed on a NovaSeq (Illumina, San Diego, CA, USA) at the Newcastle University Genomics Core Facility. Data were analyzed using the Genome Analysis Toolkit (GATK) including the variant caller MuTect2²¹⁻²³ (Broad Institute).

Illumina Infinium MethylationEPIC BeadChip array

Methylation data were generated for 18 diagnostic samples

at Eurofins Genomics (Ebersberg, Germany) using Human-Methylation Epic arrays (Illumina) and the manufacturer's standard protocols. To assess relationships between *IG-MYC-r* leukemia and other disease entities, we selected the 1,404 CpG loci previously reported to be related to B-cell maturation¹⁶ and performed *t*-distributed stochastic neighbor embedding (*t*-SNE) visualization of the combined sample set (Online Supplementary Table S3), as previously reported.²⁴

RNA-sequencing

RNA-sequencing was performed for six patients' samples at Eurofins Genomics (Ebersberg, Germany) using a TruSeq Stranded mRNA Library Prep Kit (Illumina). Data were quantified using Kallisto²⁵ and analyzed using DESeq2.²⁶ These data were compared with publicly available data (EGAS00001001795).²⁷ The top 5% of the genes with the highest median absolute deviation were selected. The resulting count matrix was used for *t*-SNE analysis.²⁸

Outcome analysis

Event-free survival (EFS) was defined as time from diagnosis to relapse, second tumor, or death, censoring at last contact. Overall survival (OS) was defined as time from diagnosis to death, censoring at last contact. For patients without data on relapse or second tumor, death was assumed to be the first event. Survival rates were calculated and compared using Kaplan-Meier methods, log-rank tests, and Cox regression models (univariate and multivariate analyses). Other comparisons were performed using the χ^2 or Fisher exact test. All tests were conducted at the 5% significance level. All outcome analyses were performed using Intercooled Stata 15.0.

Results

Demographic and clinical characterization

We collected 90 cases of BCP-ALL diagnosed by local hematologists between August 1989 and July 2019 and subsequently identified as having an *IG-MYC-r* by karyotype or FISH (Online Supplementary Figure S1, Online Supplementary Table S1). The majority were registered at diagnosis in a BCP-ALL clinical trial/registry via the UKALL group (n=32), COG (n=32) or DCOG (n=5). Eighteen additional cases were identified by international BFM study group centers, and eight of these were enrolled on ALL trials. Three further patients in whom *IG-MYC-r* was only demonstrated at relapse were not included in the survival analysis. Patients received a wide variety of trial- and clinician-determined treatments.

Among 87 cases identified at presentation, the median age at diagnosis was 10 years (range, 0-81 years) (Table 1). Fifty-two (60%) patients were male, 35 (40%) female. The

Table 1. Clinical characteristics of patients presenting at diagnosis with B-cell precursor acute lymphoblastic leukemia carrying an *IG-MYC*-rearrangement.

	All N=87	Children N=66	Adults N=21
Sex, N (%)			
Female	35 (40)	26 (39)	9 (43)
Male	52 (60)	40 (61)	12 (57)
Age in years			
Median	10	6	52
Range	0-81	0-17	20-81
White blood cell count			
N (%) of patients with >50 x 10 ⁹ /L	13/74 (18)	10/57 (18)	3/17 (18)
Median	14	14	19
Range	1.6-1200	1.6-1200	2-131
Central nervous system status, N (%)			
Positive	15 (23)	12 (22)	3 (30)
Negative	49 (77)	42 (78)	7 (70)
Not available	23	12	11
Cytogenetic risk group, N (%)			
Good risk	3 (3)	1 (1)	2 (10)
Intermediate risk	75 (86)	57 (86)	18 (86)
High risk	8 (9)	7 (11)	1 (5)
Not available	1	1	0

median presenting white blood cell count was 14x10⁹/L (range, 1.6-1200x10⁹/L, n=77 patients). Diagnostic bone marrow blast percentage was available for 64 patients and ranged from 30%-100% with a median of 86.5%. Central nervous system disease was present in 15/64 (23%) cases. Immunophenotype data were available for 33 diagnostic cases and one relapse case (*Online Supplementary Table S2*). TdT was positive in 22/29 (76%) cases. Of the TdT-negative cases, all seven (100%) were negative for surface immunoglobulin, confirming a BCP immunophenotype.

Cytogenetic characterization identified both heterogeneity and distinct genomic features

Karyotype was available for 89/90 patients (86/87 at diagnosis) and was abnormal in all cases. Three patients had high hyperdiploidy (51-65 chromosomes), a favorable risk feature and eight had high-risk genetics (*KMT2A-r*, n=6; *iAMP21*, n=1; *BCR-ABL1*, n=1) (*Table 1, Online Supplementary Table S1*). The remaining 75/86 (87%) cases were classified as intermediate cytogenetic risk at diagnosis. Fourteen patients (5 children, 9 adults) had a co-existing *BCL2-r*, one of whom also had a co-existing *BCL6-r* (*Online Supplementary Table S1*). In addition, one adult patient had only a *BCL6-r* co-existent with their *IGH-MYC-r*, identified by FISH. In the remaining 64 patients the *IG-MYC-r* was the defining cytogenetic feature.

Karyotyping and/or FISH showed that 47/90 patients (52%) had rearrangements of the *IGH* locus, 39 (43%) the *IGL* locus and three (3%) the *IGK* locus (*Figure 1A*). Two (2%) patients had *TCR-MYC-r*. One patient had both *IGH-MYC* and *IGL-MYC* rearrangements.

We estimated the percentage of cells carrying *IG-MYC-r* in 53 patients with quantitative FISH data and found that, irrespective of the *IG* locus involved, *IG-MYC-r* can be either clonal or subclonal (*Figure 1B, Online Supplementary Figure S2*). Additional evidence for the subclonal nature of some *IG-MYC-r* was derived from 3/5 *KMT2A*-rearranged cases (22901, 30611, 17659) in which karyotype and FISH data demonstrated the presence of *KMT2A*-rearranged but *MYC*-germline cells, implying that the *KMT2A*-rearranged transformation preceded the *MYC-r* (*Figure 1C, Online Supplementary Table S1*). Furthermore, it was possible to reconstruct the clonal evolution of *KMT2A*-rearranged case 17659 from the presentation and relapse metaphase data (*Figure 1D, Online Supplementary Table S1*), showing that the relapse was derived from a clone carrying the cooperating *IGL-MYC-r*. Patients with other established ALL-specific cytogenetic abnormalities (high hyperdiploidy, *iAMP21*) harbored *MYC-r* within the same clone (*Online Supplementary Table S1*). Together these data show that, for at least a proportion of cases, *IG-MYC-r* are secondary chromosomal events. Nevertheless, when compared with *MYC*-germline cases of BCP-ALL, a high level of *MYC* expression was identified, irrespective of the *IG* partner or degree of clonality (*Figure 1E*).

In nineteen patients, *IG-MYC-r* was the sole abnormality (*Online Supplementary Table S1*). Among the remaining cases, abnormalities of chromosome 1 were the most frequently observed aneuploidy/structural gain (28/89, 31%) (*Figures 1F and 2, Online Supplementary Table S1*). In the majority (25/28, 89%), 1q abnormalities were shown to be present within the same clone as the *IG-MYC-r*. One spe-

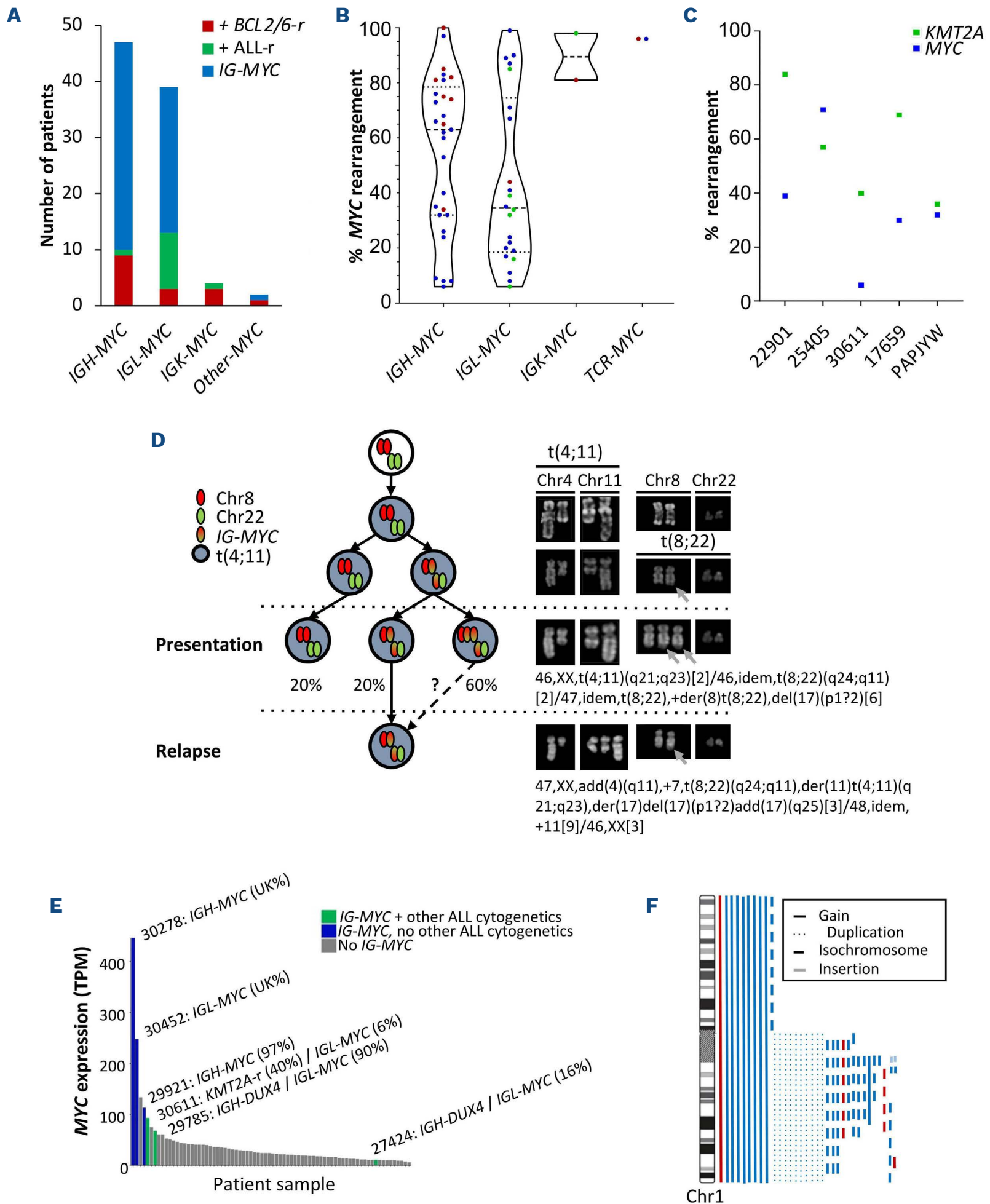


Figure 1. Cytogenetic characterization of *IG-MYC-r* patients. (A) Karyotype reveals the distribution of immunoglobulin chain involvement in *MYC* translocations (fluorescence *in situ* hybridization [FISH] data were used for one patient who presented with a normal karyotype). +*BCL2/6-r*: concomitant *BCL2/BCL6*-rearrangement; +ALL-r, concomitant established acute lymphoblastic leukemia rearrangement; *IG-MYC*: *IG-MYC* rearrangement as the defining cytogenetic abnormality. (B) Percentage of nuclei carrying *IG-MYC-r* grouped by immunoglobulin chain involvement. Blue dots, *IG-MYC-r* alone. Green dots, *IG-MYC-r* and established ALL rearrangement. Red dots, *IG-MYC-r* and *BCL2/BCL6-r*. Dotted and dashed lines, interquartile ranges. (C) Percentage rearrangement of *MYC* (blue dots) and *KMT2A* (green dots) using FISH. (D) Evolution of *t(4;11)* and subsequent gain of *t(8;22)* in case 17659. Percentages at diagnosis represent the proportion of metaphases seen with each abnormality (left panel). Representative chromosomes taken from diagnostic and relapse metaphases (right panel). Gray arrows mark the portion of chromosome 22 translocated to chromosome 8. (E) RNA sequencing comparing expression of *MYC* among (labeled) cases from the *IG-MYC-r* cohort with other in-house B-cell precursor ALL cases. TPM: transcripts per million reads. (F) Chromosomal abnormalities observed for chromosome 1 in the karyotypes of patients with *IG-MYC-r*. Red line: patients with concomitant *BCL2-r*.

cific feature we identified, which has not been recurrently described in either BL²⁹⁻³² or BCP-ALL,³³ was isochromosome of the long arm of chromosome 1, i(1)(q10). This was observed in nine patients and was associated with *IGH-MYC* in eight.

We further analyzed copy number alterations in nine of the most commonly deleted genes/regions in ALL (Figure 3) for 27 patients with sufficient DNA. Among the 15 cases with *IG-MYC-r* as the defining cytogenetic abnormality, 11 (73%) showed no deletion within the genes/regions analyzed. This is a remarkably high percentage and even more so when specifically considering pediatric patients among whom 9/10 (90%) had no deletions at diagnosis. This contrasts with just 26% of childhood ALL classified as B-other, the subgroup to which all ten patients would be assigned,¹⁹ implying an important driver role for *IG-MYC-r* in this subgroup of patients.

Finally, in order to investigate the *IG* and *MYC* breakpoints at high resolution, we used a targeted sequencing approach⁴ and were able to resolve exact breakpoints for 15/17 patients analyzed (Figures 3 and 4, *Online Supplementary Table S4*). *MYC* breakpoints differed according to *IG* partner locus. *IGH-MYC* breakpoints (n=9) were detected

5' of *MYC*, within the 5' untranslated region or within intron 1. One case had an additional breakpoint within intron 2 (Figure 4A). Each resulted in *MYC* being juxtaposed to the *IGH* super-enhancers on chromosome 14. In contrast, all *IGL-MYC* breakpoints (n=5) resulted in the translocation of the *IGL* super-enhancer 3' (telomeric) of *MYC* (Figure 4A). In patients with *IGH-MYC-r*, the majority (7/9, 78%) had breakpoints located with the V(D)J gene segments. Notably, just two patients had constant region breakpoints, more commonly associated with germinal center class switch recombination activity (Figure 4B). One of these cases also carried an *IGH-BCL2-r* (30279). In addition, this analysis identified three patients (26683, 27424 and 29785) who had cryptic *IGH-DUX4-r*,^{27,34-36} following which they were considered within the group of cases with an established ALL-specific cytogenetic abnormality (*Online Supplementary Table S1*).

Together these analyses show significant variability in the cytogenetic characteristics of BCP-ALL with *IG-MYC-r*. In some cases the *IG-MYC* recombination is clearly a secondary chromosomal event but is still capable of imparting a potentially important biological effect. In other cases it is accompanied by additional *IG* translocations,

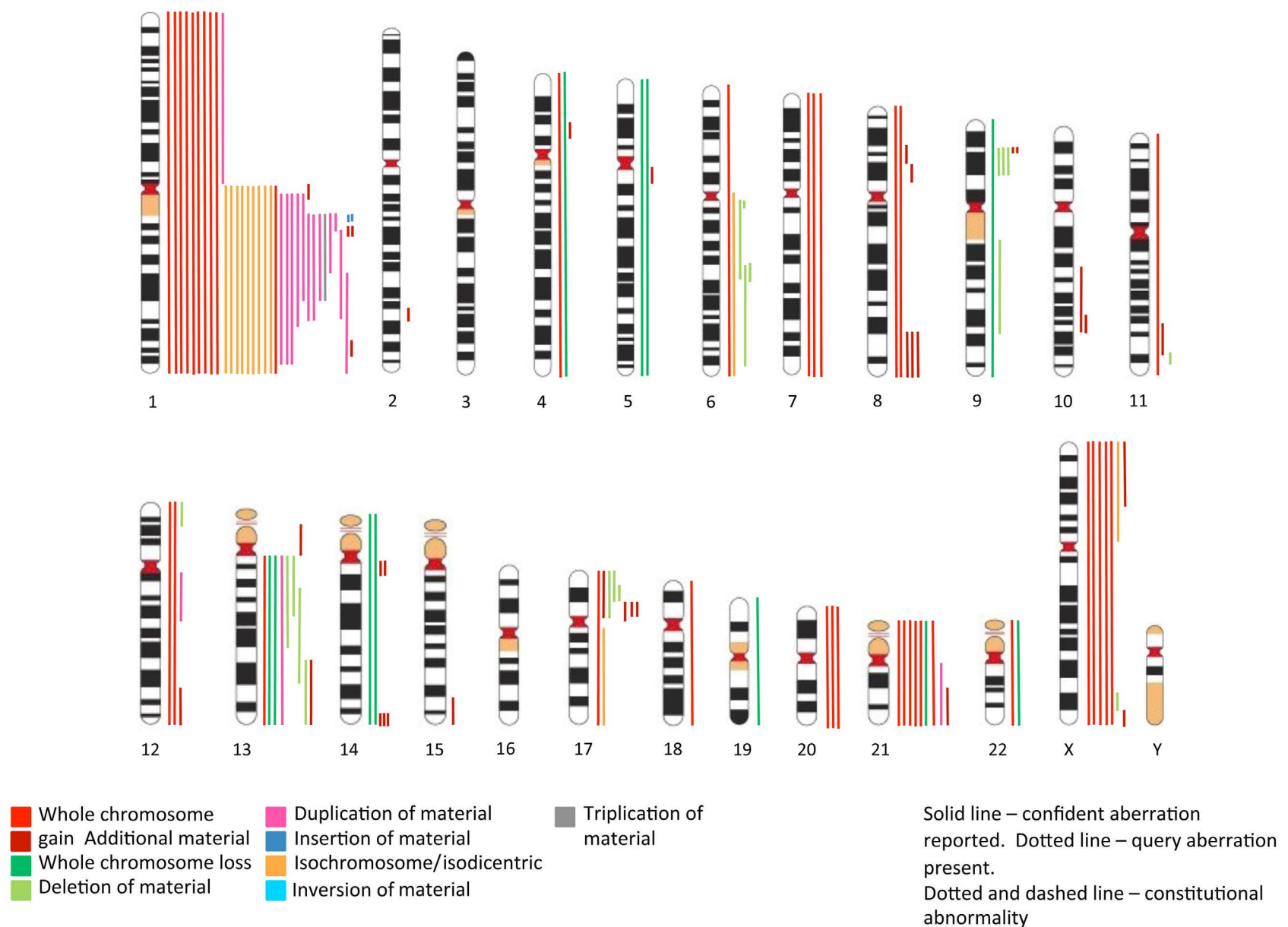


Figure 2. Ideogram of cytogenetic rearrangements reported in the karyotypes of 70 patients with *IG-MYC*-rearrangements.

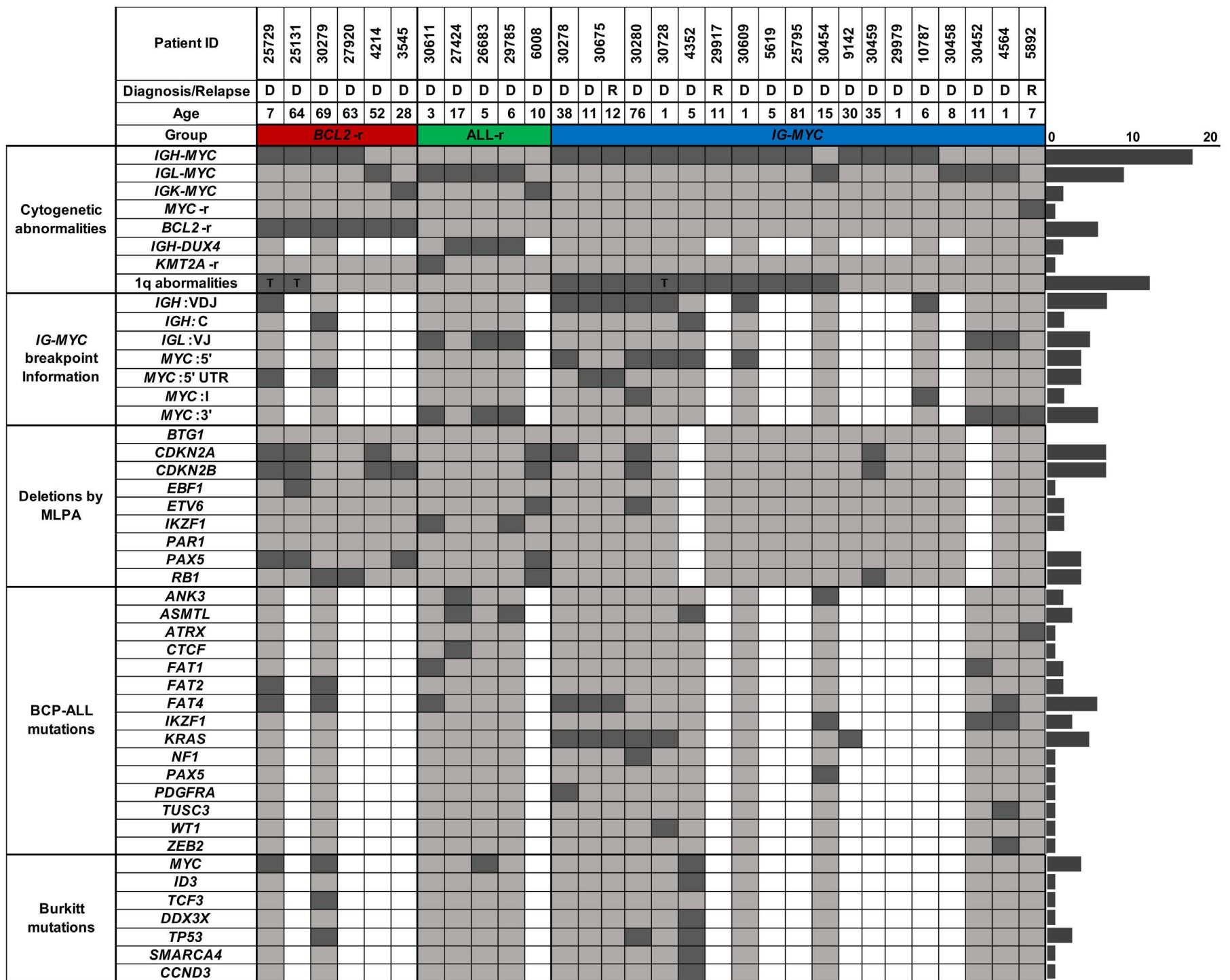


Figure 3. Oncoplot depicting the incidence of selected genomic features of *IG-MYC*-rearranged patients with material available for genomic studies. D: diagnosis; R: relapse; dark-shaded square: positive result; light-shaded square: negative result; white square: not tested; T: 1q translocation.

notably to *BCL2* and/or *BCL6*. However, in the majority of this cohort, *IG-MYC-r* occurred either in isolation or in association with additional cytogenetic features not typical of either BCP-ALL or BL. We therefore sought to investigate the relationship between these disease entities further.

***IG-MYC*-rearranged B-cell precursor acute lymphoblastic leukemias display diverse genetic, epigenetic and transcriptomic features**

In order to better characterize the molecular landscape of *IG-MYC-r* BCP-ALL we analyzed exome sequencing data from 15 diagnostic and two relapse samples, interrogating a panel of genes recurrently mutated in BCP-ALL or BL (Figure 3).^{14,37-39} In keeping with a recent analysis of exome data from five similar cases,¹⁶ we found non-synonymous

variants in *KRAS* in 5/15 (33%) patients at diagnosis. Mutations were also recurrently identified in genes mutated in BCP-ALL including, *FAT4*, *ASMTL* and *IKZF1*, observed in 6/15 (40%), 3/15 (20%) and 3/15 (20%) patients, respectively. Additional mutations were observed in *ANK3*, *FAT1*, *FAT2* (2/15, 13%) and *PDGFRA* (1/15, 7%). However, the cohort also included two patients (4352 and 30279) who harbored BL hotspot mutations in *ID3* (L64F) and *TCF3* (N554K) (*Online Supplementary Figure S3*), respectively, and additional characteristic BL mutations in *DDX3X*, *SMARCA4*, and *CCND3*. Interestingly, case 30279 also had *IGH-BCL2* and *BCL6* rearrangements as have recently been described in a cohort of high-grade, molecular BL.⁴⁰ Wagener *et al.* were also able to analyze the methylome of two cases, neither of which carried an *IG-BCL2/BCL6* rearrangement, and found these to be distinct from that

of BL, instead clustering with BCP-ALL cases.¹⁶ Here, we integrated 18 of our cases with published DNA methylation data of BCP-ALL⁴¹⁻⁴³ and BL^{16,44} cases and identified four clusters (Figure 5A). The biggest, in which no *IG-BCL2/BCL6* rearrangement or ALL-specific cytogenetic abnormality was identified (cluster A), contained seven cases (4 with *IGH-MYC-r*, 2 with *IGL-MYC-r* and 1 with *TRA-MYC-r*) and appeared most closely associated to BCP-ALL with the *TCF3-PBX1* fusion gene. Distinct from cluster A, three patients clustered with cell lines and primary samples from BL patients (cluster B). These three patients carried either BL-like mutations in

ID3/TCF and *IGH* constant region breakpoints (30279 and 4352) and/or *IG-BCL2-r* (30279 and 25729). Cluster C contained three cases identified by targeted *IG*-sequencing to have *IGH-DUX4*. Patient 30611 had a *KMT2A-r* in 40% of nuclei and clustered with other *KMT2A*-rearranged samples.

Furthermore, transcriptome analysis was conducted for six patients (5 with methylation data) for whom RNA was available (Figure 5B, C). Patients with *IG-MYC-r* and no *IG-BCL2/BCL6-r* or ALL-specific cytogenetic abnormality again associated, although here they were less close to BCP-ALL samples with *TCF3-PBX1*. Two *IGH-DUX4* pa-

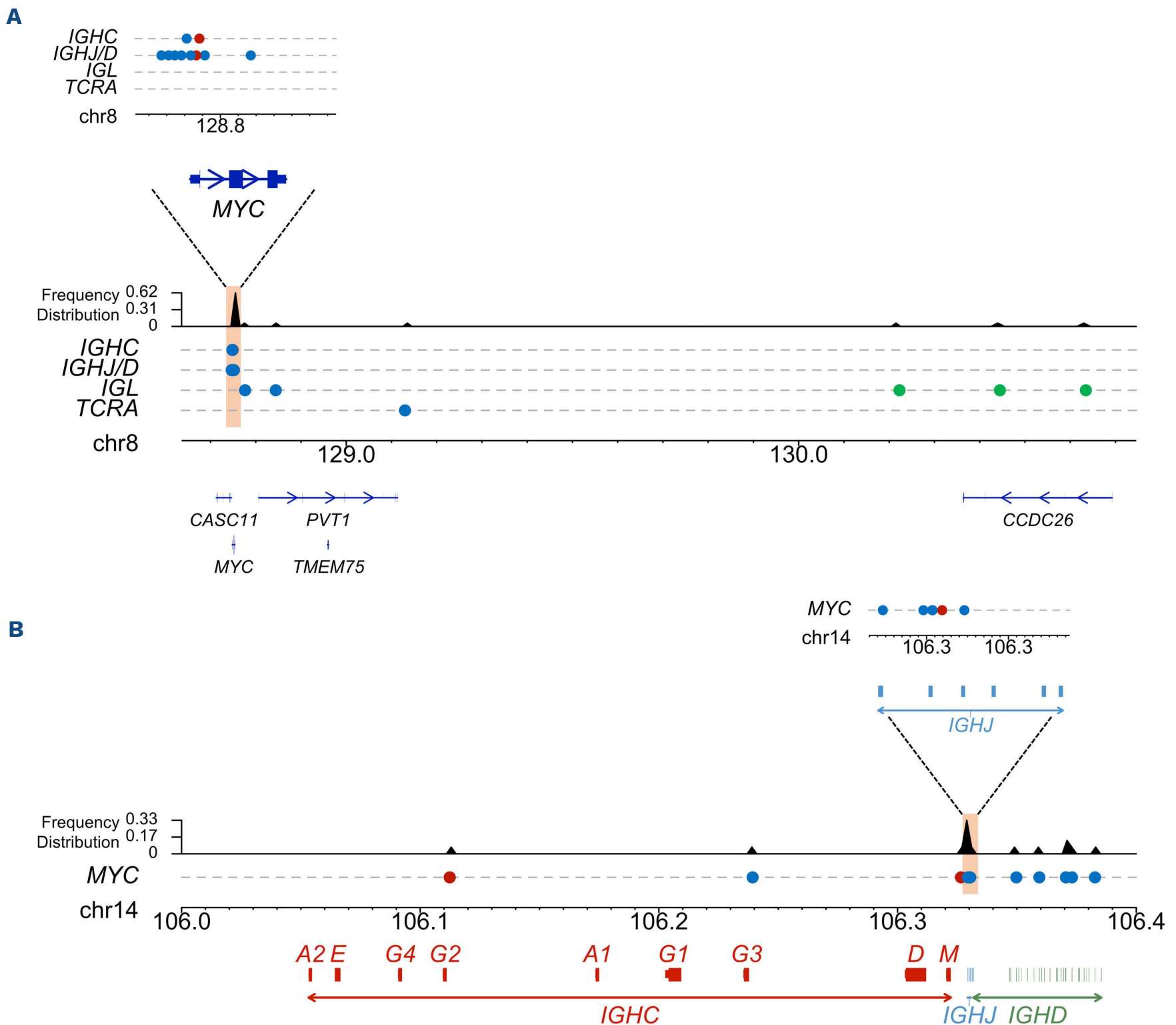


Figure 4. Targeted *IG* and *MYC* sequencing identified heterogeneous breakpoints. (A) Distribution of breakpoints within the *MYC* locus. (B) Distribution of breakpoints within the *IGH* locus. Each line shows the breakpoints for patients with translocations involving individual genomic loci. Frequency distribution defines a region of increased frequency of breaks (peach shaded area). Upper panels provide an expanded view of the breakpoint hotspots. Each dot represents an individual breakpoint. Blue dots: *IG-MYC*-rearrangement alone. Green dots, *IG-MYC*-rearrangement and established acute lymphoblastic leukemia rearrangement. Red dots, *IG-MYC*-rearrangement and *BCL2/BCL6*-rearrangement.

tients (27424 and 29785) were confirmed to cluster with published *IGH-DUX4* samples, despite substantially different *MYC-r* frequencies of 16% and 90%, respectively. *KMT2A-r* patient 30611 associated with published *KMT2A-r* patients.

Overall these analyses show that the four cases with an ALL-specific cytogenetic abnormality clustered with the relevant leukemic subgroup. In our methylome analysis, cases with either an additional *BCL2/BCL6-r*, *IGH* constant region break or a mutational profile in keeping with BL, clustered with BL. However, cases without *BCL2/BCL6-r*

or a BL-like profile formed a distinct cluster, strongly indicating they are a subtype of BCP-ALL.

Outcome of patients with *IG-MYC*-rearranged B-cell precursor acute lymphoblastic leukemia

Our genomic analysis identified three groups of *IG-MYC-r* cases, defined by: (i) concomitant *BCL2/BCL6-r*; (ii) co-occurrence of an established ALL-specific cytogenetic abnormality; and (iii) *IG-MYC-r* in the absence of another defining cytogenetic abnormality (Figure 6). That analysis demonstrated at least a proportion of *IG-MYC/IG-*

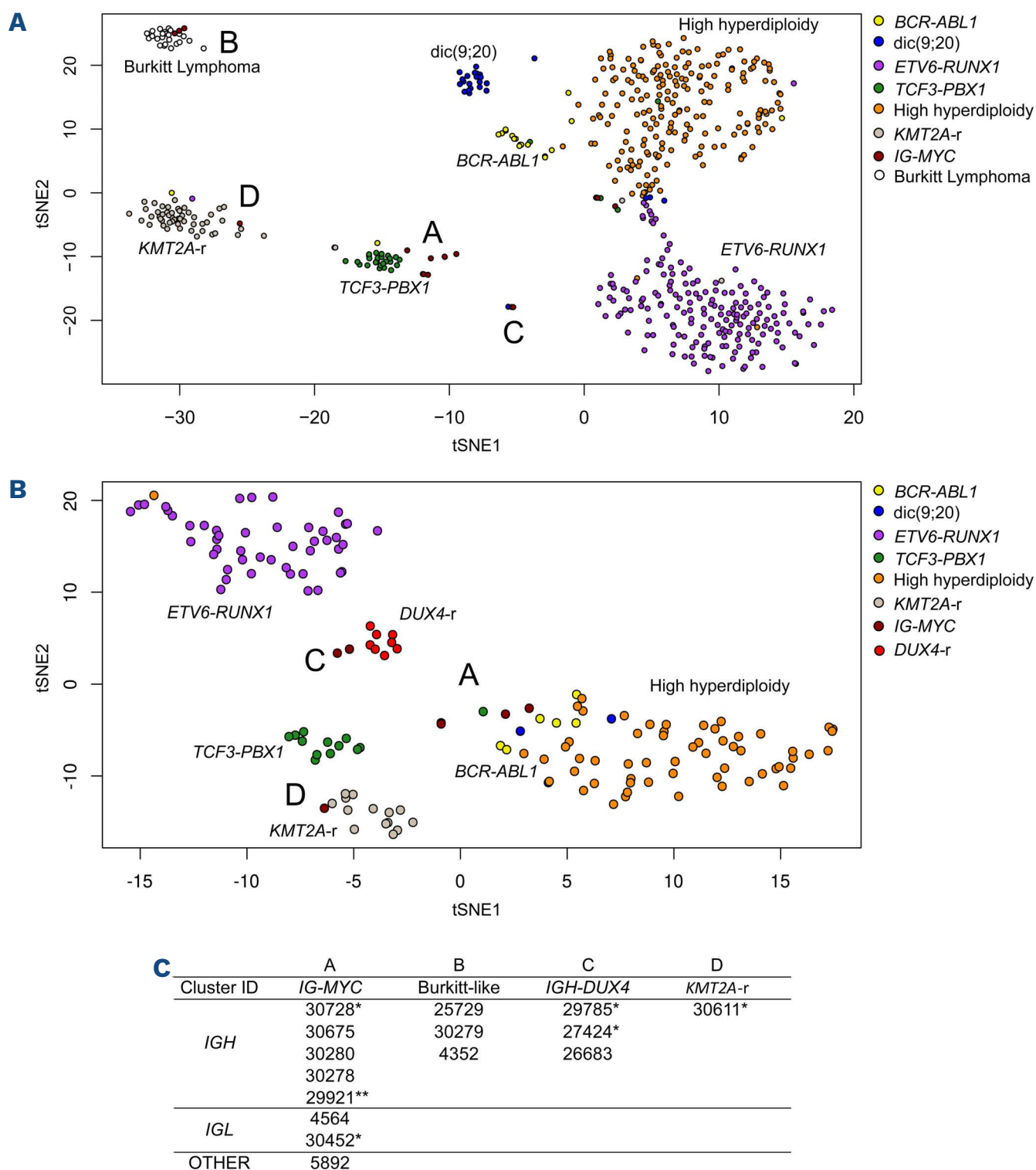


Figure 5. Methylation and transcriptome data identified five clusters within the cohort of patients with *IG-MYC*-rearrangements.

(A) Consensus clustering of methylation data. Common *t*-distributed stochastic neighbor embedding (*t*-SNE) visualization of *IG-MYC*-rearranged patients combined with publicly available data for subtypes of B-acute lymphoblastic leukemia (GSE49031, GSE69229, GSE76585), a patient with Burkitt lymphoma (GSE114210) and cell line samples (GSE92378). Each dot represents an individual patient. (B) Consensus clustering of RNA-sequencing data. Common *t*-SNE visualization of *IG-MYC*-rearranged patients combined with publicly available RNA-sequencing data for subtypes of B-acute lymphoblastic leukemia (EGAS00001001795). Each dot represents an individual patient. (C) Patients' identities assigned to clusters. *Methylation and RNA-sequencing data, **RNA-sequencing only.

BCL2/BCL6-r “double/triple hit” cases to be biologically distinct from BCP-ALL, instead showing overlap with molecular BL as has recently been described.⁴⁰ In keeping with published case reports,^{45,46} we identified a markedly inferior EFS (hazard ratio [HR]=3.10, 95% confidence interval [95% CI]: 1.42–6.76, $P=0.004$) and OS (HR=3.78, 95% CI: 1.63–8.79, $P=0.002$) in comparison to *BCL2* wildtype cases. We therefore excluded these cases from subsequent analyses.

For those cases with an ALL-specific cytogenetic abnormality, the *IG-MYC-r* was often subclonal and DNA methylation/transcriptomic analysis confirmed that they continued to cluster according to the underlying cytogenetic subgrouping. We believe that these cases present less of a diagnostic challenge and should continue to be eligible for inclusion in ALL clinical trials.

We therefore further investigated the clinical course of the diagnostically more challenging patients in whom *IG-MYC-r* represented the only recurrent cytogenetic feature. Among 59 cases enrolled in an ALL clinical trial/registry, follow-up data were available from 55 patients. However, only 20 patients (15 children and 5 adults) received the full

protocol on trial (*Online Supplementary Figure S1*). The remaining patients received unknown off-trial treatment, which was at the clinical team’s discretion. As a result, these off-trial patients had markedly shorter follow-up available, particularly with regard to relapse events (*Figure 7*). Within the small subcohort suitable for analysis, we did not identify a survival difference between children treated on an ALL trial versus those taken off an ALL trial with 3-year EFS being 47% (21–69) versus 67% (37–85) ($P=0.13$) and OS being 60% (32–80) versus 80% (50–93) ($P=0.15$), respectively. Although there were long-term survivors among trial and non-trial patients, the predominant feature among both children and adults was a high frequency of early relapse, consistent with high-risk disease (*Figure 7A, B*). Insufficient minimal residual disease data were available to allow analysis.

Twenty-six children demonstrated a molecular feature identified within our study (*IG-MYC-r* clonality >50%, *KRAS* mutation, abnormal chromosome 1 or *i(1)(q10)*) (*Online Supplementary Figure S4*). Univariate analysis did not identify any of these to be associated with EFS or OS (*Online Supplementary Table S5*).

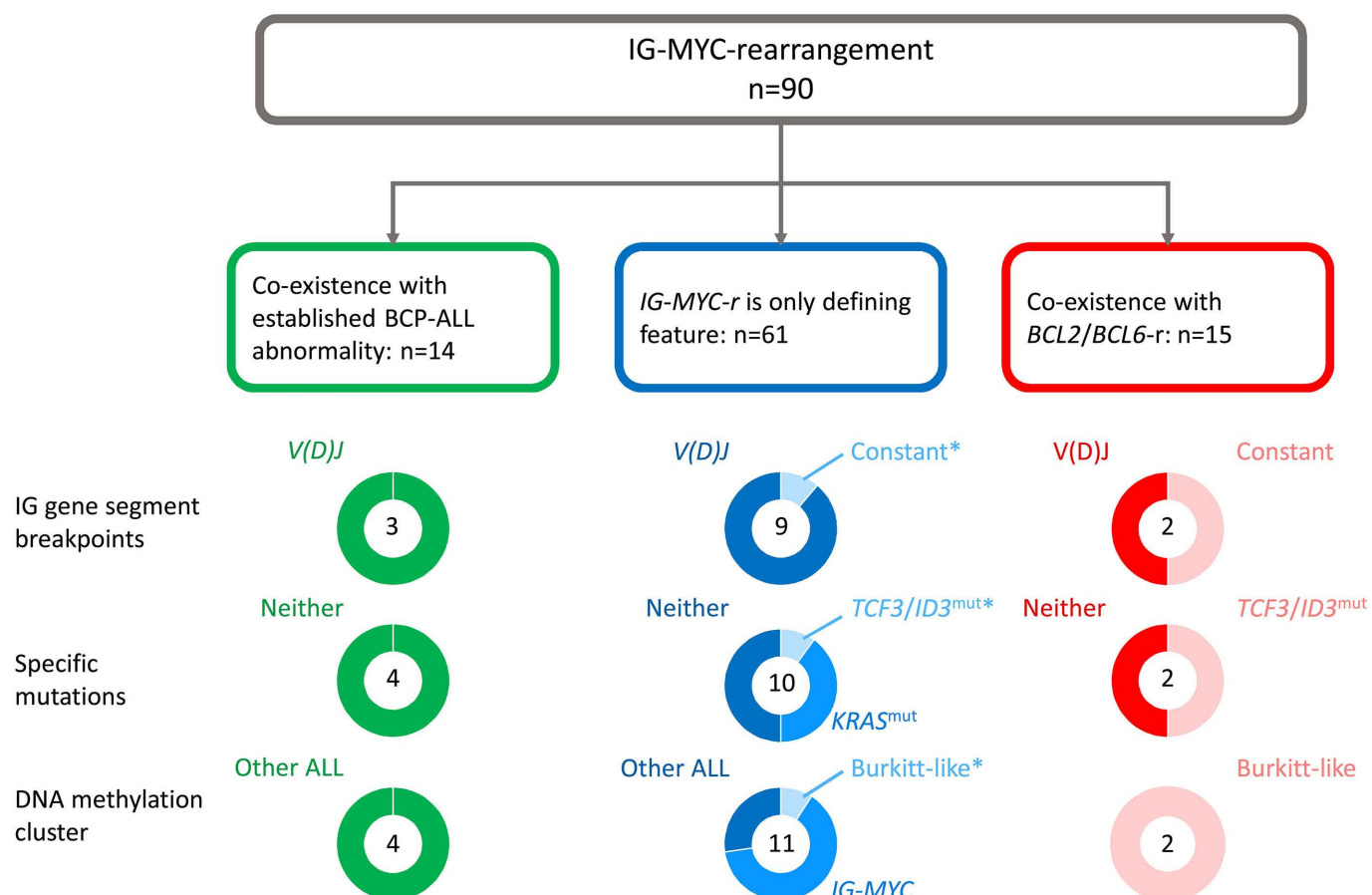


Figure 6. Molecular characteristics of cases of *IG-MYC-r* rearranged acute lymphoblastic leukemia. Summary of three groups defined within the molecular analysis. Cases with a co-existing acute lymphoblastic leukemia (ALL)-specific cytogenetic abnormality are shown in green in the left panel. Cases with an *IG-MYC-r* rearrangement (*IG-MYC-r*) as the only recurrent cytogenetic feature are shown in blue in the center panel and cases with a co-existing rearrangement of *BCL2* and/or *BCL6* are shown in red in the right panel. Each donut plot shows the proportion of cases studied which have a specific molecular feature. The total number of cases in each study is shown within each donut. The upper donut plots show the proportion with variable *V(D)J* gene segment breakpoints (dark segments) and constant segment breakpoints (light segments). The middle donut plots show the proportion of cases with either Burkitt-like *TCF3/ID3* mutations (light segments), *KRAS* mutations (medium segments) or neither such mutation (dark segments). The lower donut plots show the proportion of cases within each of three DNA methylation clusters, either Burkitt-like cluster B (light segments), the *IG-MYC-r* cluster A (medium segments) or one of the other ALL specific clusters (dark segments). *The single case in the center panel harboring both a constant region breakpoint and an *ID3* mutation (case 4352) clustered with Burkitt lymphoma/leukemia cases in our DNA methylation analysis.

Discussion

Although rare, the identification of an *IG-MYC-r* in the karyotype of patients diagnosed with BCP-ALL challenges diagnostic and clinical decision-making, with many case reports/series demonstrating the lack of uniform management, often involving hybrid ALL/B-NHL treatment.^{17,18,46} Furthermore, given the poor outcome of non-lymphoblastic/Burkitt leukemia treated with ALL therapy,^{47,48} several ALL clinical trials have excluded patients with *IG-MYC-r*, restricting the development of effective protocols. To address this clinical need we have collected the largest published cohort of *IG-MYC-r* BCP-ALL cases, from the UK, Europe and the USA, studying their molecular biology and clinical outcome.

The principal molecular distinction required is from Burkitt leukemia/lymphoma, which shares the hallmark cytogenetic feature of an *IG-MYC-r*. However, the majority (approximately 80%) of BL cases have an *IGH-MYC-r*, while the remainder have *IGL* or *IGK* rearrangements in similar proportions.⁴⁹ In contrast, we identified a much higher frequency of light chain rearrangements and particularly *IGL-MYC-r*. A substantial proportion of BCP-ALL cases harbored subclonal *IGH* or *IGL* rearrangements whereas in BL *IG-MYC-r* is considered a founder oncogenic event and is therefore clonal. We also identified recurrent *i(1)(q10)*. While gains of 1q are the most common abnormality in BL, *i(1)(q10)* has not been previously reported in that disease.²⁹⁻³² Equally, we identified only two non-*IG-MYC-r* patients with *i(1)(q10)* within the Leukaemia Research Cytogenetics Group (LRCG) database of >12,000 cases of BCP-ALL and while a recently published cohort of ALL had two cases with *i(1)(q10)* among 18 identified as harboring a *BCL2/BCL6/MYC-r*, only two other cases with *i(1)(q10)* were seen among the remaining 1,970 cases.¹⁴ Interestingly, isolated cases of immunophenotypically immature BCP-ALL with *IG-MYC-r* and *i(1)(q10)* have been reported previously.^{11,16} While these data support a specific role for *i(1)(q10)* in BCP-ALL with *IG-MYC-r* with or without *IG-BCL2-r*, the biological implications of this specific finding are unknown. Our mutational analysis of cases confirmed recurrent *KRAS* mutations within this group^{14,16} and identified additional recurrent mutations in the BCP-ALL-related genes *IKZF1* and *ASMTL*.

Targeted sequencing of the *IGH* locus identified breakpoints predominantly within the V(D)J gene segments. This contrasts with germinal center-derived malignancies, including BL, in which just 9-19% of cases carry a V(D)J gene segment breakpoint with rearrangements instead predominantly affecting the constant/switch regions.⁴⁹⁻⁵³ While our DNA methylation/transcriptome analyses were able to cluster cases with their underlying cytogenetic aberration (*KMT2A-r* or *IGH-DUX4*) when present, other *IG-MYC-r* cases with V(D)J gene segment breakpoints formed

a separate cluster distinct from BL. In just two cases we identified *IGH* constant region breakpoints, co-occurring with the only examples in our study of typical BL-related mutations in *ID3/TCF3*, *DDX3X*, *SMARCA4* and *CCND3*.³⁷⁻³⁹ Furthermore, one of these two cases also had an *IG-BCL2-r*. DNA methylation analysis clustered all three cases displaying either *IGH* constant region breakpoints and/or *IG-BCL2-r* with BL cases/cell lines, in keeping with the recently described occurrence of *BCL2-r* in adult molecular BL.⁴⁰ However, these findings contrast with a subgroup of *BCL2/BCL6/MYC* rearranged ALL which were recently described to cluster together by RNA-sequencing analysis.¹⁴ Whether this relates to alternative experimental approaches/comparators, immunophenotypic inclusion criteria or in fact further demonstrates heterogeneity within this group of patients remains unclear. However, the recent publication of the clinical outcome of this subgroup further supports the dismal prognosis associated with *BCL2/BCL6-r* ALL.⁵⁴ Whether *BCL2/BCL6-r* identifies a different disease from the majority of cases of *IG-MYC-r* BCP-ALL remains to be determined but neither published data nor the data presented here support the treatment of these patients with standard BCP-ALL therapy (Figure 7C).

Given the inconsistent treatment protocols and poor follow-up associated with patients not enrolled on a clinical trial, we sought to define patients suitable for ALL therapy for whom inclusion in prospective clinical trials would offer standardized risk-stratified, response-adapted therapy with analysis of long-term follow-up data. The inclusion of cases with BCP-ALL and an ALL-specific cytogenetic abnormality is, we believe, uncontroversial. Nonetheless, the presence of a *MYC-r* in these cases is bound to generate questions and therefore clinical trial inclusion/exclusion criteria need to be definitive. More challenging are cases in which *IG-MYC-r* is the only defining cytogenetic abnormality. Historically, these patients' outcome has been very poor, but the very few data that exist predominantly predate minimal residual disease analysis and response adaptation. With small numbers of patients in both the group remaining on an ALL trial and those removed from trial to receive therapy for which the details are not available, we did not observe a significant difference in EFS or OS. While there was a non-significant trend towards improved outcome for those removed from trial protocol therapy, the impact of heterogeneous clinician-determined therapies was unclear. These therapies are likely to have included ALL or BL protocols but also hybrid treatments delivering intensified early "BL-type" therapy with subsequent addition of ALL maintenance chemotherapy.^{17,18} These limited data underscore the need for a prospective analysis of outcome using a standardized protocol.

The rarity of the cases makes it unfeasible to conduct a

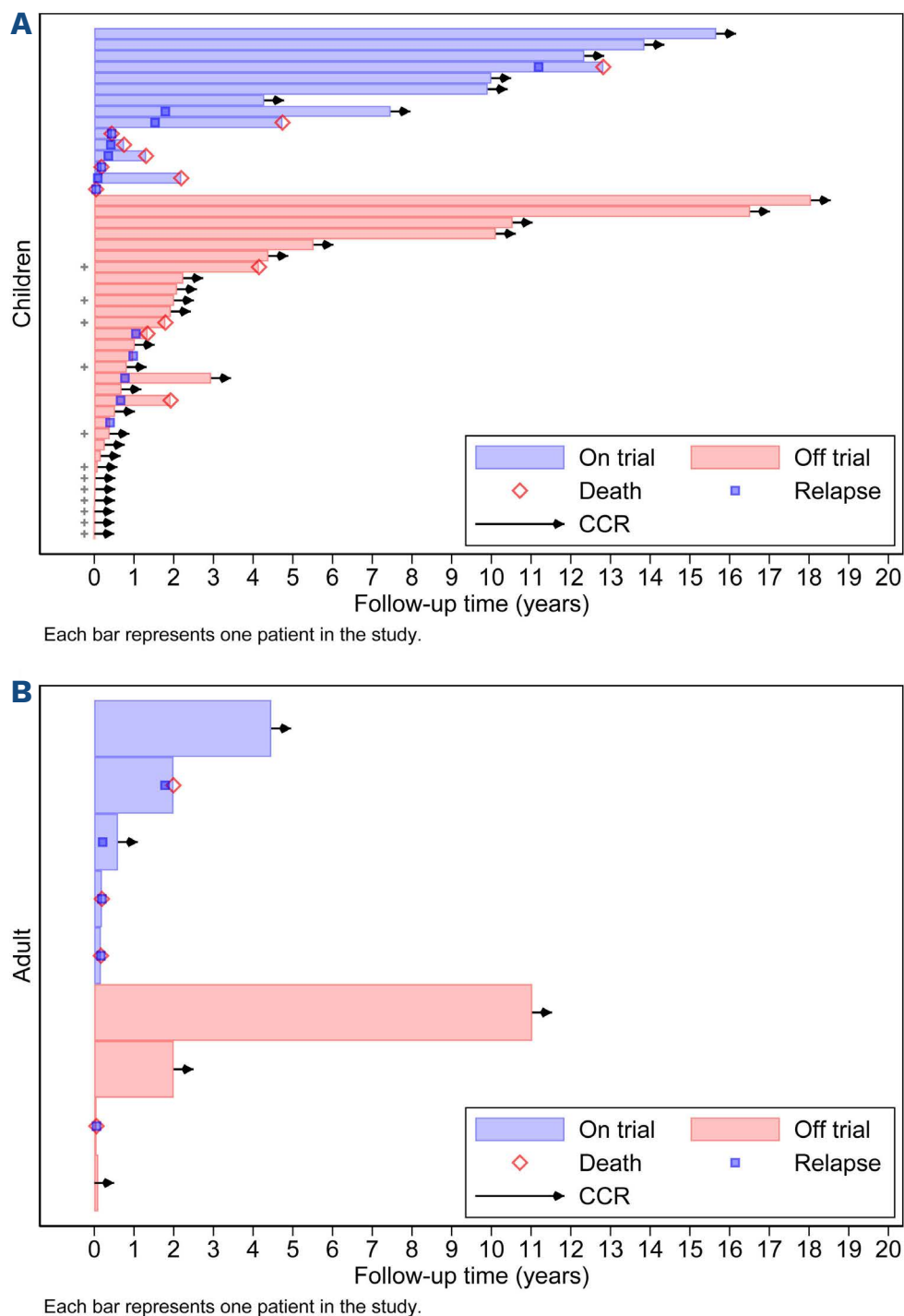


Figure 7. Swimmer plots displaying event-free survival and overall survival. (A) Children and (B) adults with *IG-MYC*-rearrangements but no other acute lymphoblastic leukemia-specific cytogenetic abnormality. Suggested approach for the assignment of patients to a treatment strategy (C). + For patients without data on relapse or second tumor, death was assumed to be the first event. ALL: acute lymphoblastic leukemia; BCP: B-cell precursor; CCR: continuous complete remission; sIG: surface immunoglobulin.

dedicated trial solely for these patients. Currently they are being lost to investigation and receive therapy of unproven efficacy resulting in outcomes significantly inferior to those of standard ALL or BL. We believe that the underlying biology of these *IG-MYC-r* patients indicate that they are part of the ALL spectrum. To improve our understanding of this BCP-ALL subtype and patients' outcome, we strongly suggest that they be included in clinical trials able to prospectively measure early treatment response, supporting informed decision-making on whether to continue a standard treatment strategy or not. Those with very poor response to initial therapy may be considered for alternative therapies, similar to the approach to acute leukemia of ambiguous lineage being taken by some study groups.^{55,56}

Within that setting, use of disease-agnostic approaches such as antibody or advanced cellular therapies, may be logical.

In summary, we have demonstrated that surface immunoglobulin-negative BCP-ALL with *IG-MYC-r* are a high-risk subgroup of BCP-ALL. Optimal treatment can only be determined by removing barriers to treating patients with uniform therapy and collection of detailed long-term clinical follow-up data. We believe that clinical trial protocols should not exclude these patients, who should in fact be given access to contemporary, risk-stratified, response-adapted therapy.

Disclosures

No conflicts of interest to disclose.

Contributions

SB, LJR, FWvD and AVM conceived and designed the study; SB, YD, AA, YB, JB, BB, GAAB, GC, GG, HAdG, CH, LLN, MP, AP, ESe, ESo, SS, VHJvdV, VR, SPH, CJH, FWvD, MLL, JV, AVM and LJR provided clinical data and contributed patient samples; SB, ECS, AM, MZ, KTMF, MB, HL, LJ, NK, EW, CA, CMB, BAW, AVM and LJR performed experiments and analyzed experimental data; AE and YD collected and analyzed outcome data; SB, LJR and AVM wrote the manuscript with additional contributions from MLL, JM and JV; all co-authors contributed to manuscript review and editing and approved the final manuscript for submission.

Acknowledgments

We would like to thank patients and their families for donating their samples for research and each of the institutional/national BioBanks for providing those samples for this study, including the Blood Cancer UK Childhood Leukaemia Cell Bank. We thank Adele Fielding for help in identifying UK patients.

Funding

We would like to thank those who provided financial support. Kay Kendall Leukaemia Fund (KKL515), Wellcome Trust Institutional Strategic Support Fund (204787/Z/16/Z), The Newcastle upon Tyne Hospitals NHS charity and KidsCan

Children's Cancer Research and The Little Princess Trust (to LJR). LJR held a Newcastle University Research Fellowship and A.M. a Newcastle University Faculty Fellowship. SB was supported by The Sir Bobby Robson Foundation and an MRC Clinician Scientist Fellowship MR/S021590/1. COG funding was available through U10 CA98413 and U10 CA180899 (COG Statistics and Data Center grants), U24 CA114766 and U24-CA196173 (COG Specimen Banking). AVM and CJH were supported by Blood Cancer UK (15036) and Cancer Research UK (A21019, Moorman and Fielding). LLN was partially supported by MFAG 2009 – AIRC (Italian Association for Cancer Research) (Lo Nigro). VR was supported by a Bloodwise (formerly Leukaemia and Lymphoma Research) Senior Bennett Fellowship (#12005), the JGW Patterson Foundation and the Little Princess Trust. MZ was supported by North East Promenaders. GC was supported by the Italian Association for Cancer Research (Grant n.IG17593) and Comitato Maria Letizia Verga.

Data-sharing statement

All previously publicly available datasets used are referred to in the Methods section and in Online Supplementary Table S3. Methylation data are available from the GEO repository under accession number GSE174248. RNA, whole exome and targeted sequencing data are available from the EGA repository under EGA study ID EGAS00001005111.

References

- Klapper W, Stoecklein H, Zeynalova S, et al. Structural aberrations affecting the MYC locus indicate a poor prognosis independent of clinical risk factors in diffuse large B-cell lymphomas treated within randomized trials of the German High-Grade Non-Hodgkin's Lymphoma Study Group (DSHNHL). *Leukemia*. 2008;22(12):2226-2229.
- Savage KJ, Johnson NA, Ben-Neriah S, et al. MYC gene rearrangements are associated with a poor prognosis in diffuse large B-cell lymphoma patients treated with R-CHOP chemotherapy. *Blood*. 2009;114(17):3533-3537.
- Ott G, Rosenwald A, Campo E. Understanding MYC-driven aggressive B-cell lymphomas: pathogenesis and classification. *Blood*. 2013;122(24):3884-3891.
- Mikulasova A, Ashby C, Tytarenko RG, et al. Microhomology-mediated end joining drives complex rearrangements and overexpression of MYC and PVT1 in multiple myeloma. *Haematologica*. 2020;105(4):1055-1066.
- Swerdlow SH, Campo E, Harris NL, et al. WHO Classification of Tumours of Haematopoietic and Lymphoid Tissues (Revised 4th edition): International Agency for Research on Cancer (IARC). 2017
- Navid F, Mosijczuk AD, Head DR, et al. Acute lymphoblastic leukemia with the (8;14)(q24;q32) translocation and FAB L3 morphology associated with a B-precursor immunophenotype: the Pediatric Oncology Group experience. *Leukemia*. 1999;13(1):135-141.
- Loh ML, Samson Y, Motte E, et al. Translocation (2;8)(p12;q24) associated with a cryptic t(12;21)(p13;q22) TEL/AML1 gene rearrangement in a child with acute lymphoblastic leukemia. *Cancer Genet Cytogenet*. 2000;122(2):79-82.
- Reid MM, Drewery C, Windebank KP. Surface immunoglobulin-negative acute lymphoblastic leukaemia with predominant L1 morphology, occasional L3 cells and t(8;22). *Br J Haematol*. 2003;122(5):693.
- Gupta AA, Grant R, Shago M, Abdelhaleem M. Occurrence of t(8;22)(q24.1;q11.2) involving the MYC locus in a case of pediatric acute lymphoblastic leukemia with a precursor B cell immunophenotype. *J Pediatr Hematol Oncol*. 2004;26(8):532-534.
- Meeker ND, Cherry AM, Bangs CD, Kimble Frazer J. A pediatric B lineage leukemia with coincident MYC and MLL translocations. *J Pediatr Hematol Oncol*. 2011;33(2):158-160.
- Roug AS, Wendtland P, Bendix K, Kjeldsen E. Supernumerary isochromosome 1, idic(1)(p12), leading to tetrasomy 1q in Burkitt lymphoma. *Cytogenet Genome Res*. 2014;142(1):7-13.
- Sato Y, Kurosawa H, Fukushima K, Okuya M, Arisaka O. Burkitt-type acute lymphoblastic leukemia with precursor B-cell immunophenotype and partial tetrasomy of 1q: a case report. *Medicine (Baltimore)*. 2016;95(10):e2904.
- Meznarich J, Miles R, Paxton CN, Afify Z. Pediatric B-cell lymphoma with lymphoblastic morphology, TdT expression, MYC rearrangement, and features overlapping with Burkitt lymphoma. *Pediatr Blood Cancer*. 2016;63(5):938-940.
- Gu Z, Churchman ML, Roberts KG, et al. PAX5-driven subtypes of B-progenitor acute lymphoblastic leukemia. *Nat Genet*. 2019;51(2):296-307.

15. Forestier E, Johansson B, Borgström G, Kerndrup G, Johansson J, Heim S. Cytogenetic findings in a population-based series of 787 childhood acute lymphoblastic leukemias from the Nordic countries. The NOPHO Leukemia Cytogenetic Study Group. *Eur J Haematol.* 2000;64(3):194-200.
16. Wagener R, Lopez C, Kleinheinz K, et al. *IG-MYC (+)* neoplasms with precursor B-cell phenotype are molecularly distinct from Burkitt lymphomas. *Blood.* 2018;132(21):2280-2285.
17. Herbrueggen H, Mueller S, Rohde J, et al. Treatment and outcome of *IG-MYC(+)* neoplasms with precursor B-cell phenotype in childhood and adolescence. *Leukemia.* 2020;34(3):942-946.
18. Zhang C, Amos Burke GAA. Pediatric precursor B-cell acute lymphoblastic leukemia with *MYC 8q24* translocation - how to treat? *Leuk Lymphoma.* 2018;59(8):1807-1813.
19. Schwab CJ, Chilton L, Morrison H, et al. Genes commonly deleted in childhood B-cell precursor acute lymphoblastic leukemia: association with cytogenetics and clinical features. *Haematologica.* 2013;98(7):1081-1088.
20. Chen X, Schulz-Trieglaff O, Shaw R, et al. Manta: rapid detection of structural variants and indels for germline and cancer sequencing applications. *Bioinformatics.* 2016;32(8):1220-1222.
21. Li H, Durbin R. Fast and accurate long-read alignment with Burrows-Wheeler transform. *Bioinformatics.* 2010;26(5):589-595.
22. McKenna A, Hanna M, Banks E, et al. The Genome Analysis Toolkit: a MapReduce framework for analyzing next-generation DNA sequencing data. *Genome Res.* 2010;20(9):1297-1303.
23. Cibulskis K, Lawrence MS, Carter SL, et al. Sensitive detection of somatic point mutations in impure and heterogeneous cancer samples. *Nat Biotechnol.* 2013;31(3):213-219.
24. Sharma T, Schwalbe EC, Williamson D, et al. Second-generation molecular subgrouping of medulloblastoma: an international meta-analysis of group 3 and group 4 subtypes. *Acta Neuropathol.* 2019;138(2):309-326.
25. Bray NL, Pimentel H, Melsted P, Pachter L. Near-optimal probabilistic RNA-seq quantification. *Nat Biotechnol.* 2016;34(5):525-527.
26. Love MI, Huber W, Anders S. Moderated estimation of fold change and dispersion for RNA-seq data with DESeq2. *Genome Biol.* 2014;15(12):550.
27. Lilljebjorn H, Henningsson R, Hyrenius-Wittsten A, et al. Identification of *ETV6-RUNX1*-like and *DUX4*-rearranged subtypes in paediatric B-cell precursor acute lymphoblastic leukaemia. *Nat Commun.* 2016;7:11790.
28. van der Maaten L, Hinton G. Visualising data using t-SNE. *J Mach Learn Res.* 2008;9(86):2579-2605.
29. Newman AM, Zaka M, Zhou P, et al. Genomic abnormalities of *TP53* define distinct risk groups of paediatric B-cell non-Hodgkin lymphoma. *Leukemia.* 2022;36(3):781-789.
30. Schiffman JD, Lorimer PD, Rodic V, et al. Genome wide copy number analysis of paediatric Burkitt lymphoma using formalin-fixed tissues reveals a subset with gain of chromosome 13q and corresponding miRNA over expression. *Br J Haematol.* 2011;155(4):477-486.
31. Scholtysik R, Kreuz M, Klapper W, et al. Detection of genomic aberrations in molecularly defined Burkitt's lymphoma by array-based, high resolution, single nucleotide polymorphism analysis. *Haematologica.* 2010;95(12):2047-2055.
32. Havelange V, Pepermans X, Ameye G, et al. Genetic differences between paediatric and adult Burkitt lymphomas. *Br J Haematol.* 2016;173(1):137-144.
33. Moorman AV, Ensor HM, Richards SM, et al. Prognostic effect of chromosomal abnormalities in childhood B-cell precursor acute lymphoblastic leukaemia: results from the UK Medical Research Council ALL97/99 randomised trial. *Lancet Oncol.* 2010;11(5):429-438.
34. Yasuda T, Tsuzuki S, Kawazu M, et al. Recurrent *DUX4* fusions in B cell acute lymphoblastic leukemia of adolescents and young adults. *Nat Genet.* 2016;48(5):569-574.
35. Liu YF, Wang BY, Zhang WN, et al. Genomic profiling of adult and pediatric B-cell acute lymphoblastic leukemia. *EBioMedicine.* 2016;8:173-183.
36. Zhang J, McCastlain K, Yoshihara H, et al. Deregulation of *DUX4* and *ERG* in acute lymphoblastic leukemia. *Nat Genet.* 2016;48(12):1481-1489.
37. Love C, Sun Z, Jima D, et al. The genetic landscape of mutations in Burkitt lymphoma. *Nat Genet.* 2012;44(12):1321-1325.
38. Schmitz R, Young RM, Ceribelli M, et al. Burkitt lymphoma pathogenesis and therapeutic targets from structural and functional genomics. *Nature.* 2012;490(7418):116-120.
39. Richter J, Schlesner M, Hoffmann S, et al. Recurrent mutation of the *ID3* gene in Burkitt lymphoma identified by integrated genome, exome and transcriptome sequencing. *Nat Genet.* 2012;44(12):1316-1320.
40. Bouska A, Bi C, Lone W, et al. Adult high-grade B-cell lymphoma with Burkitt lymphoma signature: genomic features and potential therapeutic targets. *Blood.* 2017;130(16):1819-1831.
41. Nordlund J, Bäcklin CL, Wahlberg P, et al. Genome-wide signatures of differential DNA methylation in pediatric acute lymphoblastic leukemia. *Genome Biol.* 2013;14(9):r105.
42. Gabriel AS, Lafta FM, Schwalbe EC, et al. Epigenetic landscape correlates with genetic subtype but does not predict outcome in childhood acute lymphoblastic leukemia. *Epigenetics.* 2015;10(8):717-726.
43. Bergmann AK, Castellano G, Alten J, et al. DNA methylation profiling of pediatric B-cell lymphoblastic leukemia with *KMT2A* rearrangement identifies hypomethylation at enhancer sites. *Pediatr Blood Cancer.* 2017;64(3):e26251.
44. Hernandez-Vargas H, Gruffat H, Cros MP, et al. Viral driven epigenetic events alter the expression of cancer-related genes in Epstein-Barr-virus naturally infected Burkitt lymphoma cell lines. *Sci Rep.* 2017;7(1):5852.
45. Liu W, Hu S, Konopleva M, et al. De novo *MYC* and *BCL2* double-hit B-cell precursor acute lymphoblastic leukemia (BCP-ALL) in pediatric and young adult patients associated with poor prognosis. *Pediatr Hematol Oncol.* 2015;32(8):535-547.
46. Sakaguchi K, Imamura T, Ishimaru S, et al. Nationwide study of pediatric B-cell precursor acute lymphoblastic leukemia with chromosome 8q24/*MYC* rearrangement in Japan. *Pediatr Blood Cancer.* 2020;67(7):e28341.
47. Anderson JR, Wilson JF, Jenkin DT, et al. Childhood non-Hodgkin's lymphoma. The results of a randomized therapeutic trial comparing a 4-drug regimen (COMP) with a 10-drug regimen (LSA2-L2). *N Engl J Med.* 1983;308(10):559-565.
48. Moorman AV, Harrison CJ, Buck GAN, et al. Karyotype is an independent prognostic factor in adult acute lymphoblastic leukemia (ALL): analysis of cytogenetic data from patients treated on the Medical Research Council (MRC) UKALLXII/Eastern Cooperative Oncology Group (ECOG) 2993 trial. *Blood.* 2007;109(8):3189-3197.
49. Grande BM, Gerhard DS, Jiang A, et al. Genome-wide discovery of somatic coding and non-coding mutations in pediatric endemic and sporadic Burkitt lymphoma. *Blood.* 2019;133(12):1313-1324.
50. Gelmann EP, Psallidopoulos MC, Papas TS, Dalla Favera R. Identification of reciprocal translocation sites within the *c-myc*

- oncogene and immunoglobulin mu locus in a Burkitt lymphoma. *Nature*. 1983;306(5945):799-803.
51. Busch K, Keller T, Fuchs U, et al. Identification of two distinct MYC breakpoint clusters and their association with various IGH breakpoint regions in the t(8;14) translocations in sporadic Burkitt-lymphoma. *Leukemia*. 2007;21(8):1739-1751.
52. López C, Kleinheinz K, Aukema SM, et al. Genomic and transcriptomic changes complement each other in the pathogenesis of sporadic Burkitt lymphoma. *Nat Commun*. 2019;10(1):1459.
53. Bendig S, Walter W, Meggendorfer M, et al. Whole genome sequencing demonstrates substantial pathophysiological differences of MYC rearrangements in patients with plasma cell myeloma and B-cell lymphoma. *Leuk Lymphoma*. 2021;62(14):3420-3429.
54. Paietta E, Roberts KG, Wang V, et al. Molecular classification improves risk assessment in adult BCR-ABL1-negative B-ALL. *Blood*. 2021;138(11):948-958.
55. Oberley MJ, Raikar SS, Wertheim GB, et al. Significance of minimal residual disease in pediatric mixed phenotype acute leukemia: a multicenter cohort study. *Leukemia*. 2020;34(7):1741-1750.
56. Orgel E, Alexander TB, Wood BL, et al. Mixed-phenotype acute leukemia: a cohort and consensus research strategy from the Children's Oncology Group Acute Leukemia of Ambiguous Lineage Task Force. *Cancer*. 2020;126(3):593-601.